Natronomicrosphaera hydrolytica, gen. nov., sp. nov., a first representative of the phylum Planctomycetota from soda lakes

Sorokin, Dimitry Y.; Merkel, Alexander Y.; Bale, Nicole J.; Koenen, Michel; Sinninghe Damste, Jaap S. ; Marturano, Laura ; Messina, Enzo; La Cono, Violetta ; Yakimov, Michail M.

DOI
10.1016/j.syapm.2025.126608

Publication date
2025

Document Version
Final published version

Published in
Systematic and Applied Microbiology

Citation (APA)
Sorokin, D. Y., Merkel, A. Y., Bale, N. J., Koenen, M., Sinninghe Damste, J. S., Marturano, L., Messina, E., La Cono, V., & Yakimov, M. M. (2025). Natronomicrosphaera hydrolytica, gen. nov., sp. nov., a first representative of the phylum Planctomycetota from soda lakes. *Systematic and Applied Microbiology*, *48*(3), Article 126608. https://doi.org/10.1016/j.syapm.2025.126608

Systematic and Applied Microbiology 48 (2025) 126608

Contents lists available at ScienceDirect

Systematic and Applied Microbiology

journal homepage: www.elsevier.com/locate/syapm

Natronomicrosphaera hydrolytica, gen. nov., sp. nov., a first representative of the phylum *Planctomycetota* from soda lakes

Dimitry Y. Sorokin [a,b,*], Alexander Y. Merkel [a], Nicole J. Bale [c], Michel Koenen [c], Jaap S. Sinninghe Damsté [c], Laura Marturano [d], Enzo Messina [d], Violetta La Cono [d], Michail M. Yakimov [d]

[a] *Winogradsky Institute of Microbiology, Research Centre of Biotechnology, Russian Academy of Sciences, Moscow, Russia*
[b] *Department of Biotechnology, Delft University of Technology, Delft, the Netherlands*
[c] *NIOZ Royal Netherlands Institute for Sea Research, Department of Marine Microbiology and Biogeochemistry, Den Burg, Texel, the Netherlands*
[d] *Institute of Polar Sciences, ISP-CNR, Messina, Italy*

ARTICLE INFO

Keywords:
Soda lakes
Hyaluronic acid
Haloalkaliphilic
Planctomycetota
Phicisphaeraceae

ABSTRACT

Despite intensive microbiological characterization of soda lake microbial communities, no culturable representatives from the phylum *Planctomycetota* have been isolated from these haloalkaline habitats. In the context of studying polysaccharide utilization by soda lake microbial communities, we used polysaccharide hyaluronic acid as enrichment substrate at aerobic, moderate haloalkaline conditions (1 M total Na^+, pH 9.5). This resulted in a selective enrichment and isolation in pure culture of a bacterial strain AB-hyl4 belonging to *Planctomycetota*. The cells are tiny motile cocci growing in large aggregates, with the Gram-negative type of ultrastructure and producing a yellow pigment. This obligate aerobic saccharolytic heterotroph has an extremely narrow growth substrate range including, besides hyaluronic acid, melezitose and glycerol. The membrane lipids consist of phosphatidylcholine and two types of neutral lipids, including hopanoids and monounsaturated C17 and C19 hydrocarbons. Phylogenomic analysis placed the isolate into the family *Phycisphaeraceae*, class *Phycisphaerae,* as a new genus-level lineage. Its genome contained a gene encoding a polysaccharide lyase from the PL8 family which is probably responsible for the degradation of hyaluronic acid to a dimer, followed by its transport and hydrolysis into monomers in periplasm and final glycolytic degradation in cytoplasm. On the basis of distinct phenotypic and genomic properties, strain AB-hyl4^T (DSM 117794 = UQM 41914) is proposed to be classified as *Natronomicrosphaera hydrolytica* gen. nov., sp. nov.

Introduction

Hypersaline soda lakes are the only aquatic habitats with a stable high pH and moderate to extreme high salinity due to a presence of molar concentrations of soluble sodium carbonate/bicarbonate alkalinity buffer creating selective conditions for domination of obligate haloalkaliphilic prokaryotes. They have been intensively studied during the last several decades in soda lakes located in Central Asia (southern Siberia, north-eastern Mongolia and Inner Mongolia), East African Rift Valley, California and Nevada (USA) and British Columbia in Canada (Jones, 1977; Schagerl, 2016). Culturing and molecular ecology investigations revealed taxonomically diverse microbial communities active in carbon, sulfur and nitrogen cycling present in these soda lakes (Grant and Jones, 2016; Sorokin, 2017; Sorokin et al., 2014; Sorokin et al., 2015a; Vavourakis et al., 2016, 2018; Zorz et al., 2019; Haines et al., 2023).

Our recent studies on the functional microbiology of hypersaline soda lakes focused on the study of the unrecognized polysaccharidolytic potential of extremely halophilic natronoarchaea. This yielded a range of natronoarchaeal isolates capable of growth with chitin, cellulose and many other polysaccharides based on neutral sugars (Sorokin et al., 2015b; Sorokin et al., 2018; Sorokin et al., 2019; Elcheninov et al., 2023). However, extremely halophilic natronoarchaea seemed not to be using acidic polysaccharides as a substrate. Therefore, attempts continued at moderate salinity to probe for the presence of acidic polysaccharides-utilizing bacteria in soda lakes. The use of sodium hyaluronate (a linear heteropolymer of *N*-acetylglucosamine and glucuronic acid) as a substrate, resulted in a selective enrichment and

* Corresponding author at: Winogradsky Institute of Microbiology, Research Centre of Biotechnology, Russian Academy of Sciences, Moscow, Russia.
E-mail address: soroc@inmi.ru (D.Y. Sorokin).

https://doi.org/10.1016/j.syapm.2025.126608
Received 4 February 2025; Received in revised form 16 April 2025; Accepted 22 April 2025
Available online 28 April 2025

isolation in pure culture of a haloalkaliphilic bacterium belonging to the phylum *Planctomycetota*. Their presence in soda lakes has, so far, only been detected by molecular ecology methods. For example, MAGs belonging to *Phycisphaerales* were assembled from surface sediments of southeastern Siberian and Canadian soda lakes, where they accounted for up to 2 % of the prokaryotic community (Vavourakis et al., 2016, 2018, 2019; Zorz et al., 2019). Here we describe the phenotypic, the phylogenomic and the functional genomic properties of this bacterium and propose to classify the isolate as a new genus and species within the class *Phycisphaerae* of the phylum *Planctomycetota*.

Materials and methods

Inoculum, enrichment conditions and isolation of pure culture

The top 1–2 cm layer of oxic sediments and near-bottom brines were collected by a 50 ml syringe from six moderately saline soda lakes located in the south of Kulunda Steppe (Altai region, Russia) in July 2022. The salt concentration of the brines ranged from 50 to 150 g l^{-1}, the pH from 10.1 to 10.6 and the carbonate alkalinity from 0.5 to 1.8 M. The individual samples were mixed in equal proportions in a 50 ml Falcon tube, homogenized by vigorous shacking and incubated statically for 1 h to allow precipitation of coarse heavy particles. The residual top 10 ml fraction containing fine particle suspension was then used as an inoculum (5 % *v*/v).

The enrichment medium was based on sodium carbonate/bicarbonate buffer containing 0.9 M total Na^+ as carbonates, 0.1 M NaCl, 1 g l^{-1} K_2HPO_4 and 20 mg l^{-1} yeast extract (final pH of 9.5 after autoclaving at 120 °C). After sterilization, the base medium was supplemented with 1 mM Mg sulfate, 4 mM NH_4Cl and 1 ml each of trace metal and vitamin mix according to Pfennig and Lippert (1966). Finally, 1 g l^{-1} of 2 MDa sodium hyaluronate (Hyl) (Biosynth, Bratislava, Slovakia) from 2 % (*w*/*v*) stock solution was added as the carbon and energy source. Twenty ml enrichment was incubated at 30 °C on a rotary shaker at 120 rpm in 100 ml screw cap bottles until visible microscopic evidence of bacterial growth (after settling of sediment particles by a brief low-speed centrifugation). Those was passed two times at 1:100 dilution to obtain a sediment-free culture which was further purified by serial dilutions up to (10^{-10}) in the same medium. Several consecutive series were positive up to (10^{-8}) dilution dominated by tiny cocci in clumps, which made final purification in liquid medium inefficient. Attempts of surface plating from the maximum dilutions showed no growth. However, an alternative plating method (used for anaerobes) in agar-shake mode inside soft agar (0.8 % *w*/*v* final, poured into plates) allowed to obtain separate colonies of the target bacterium after preliminary additional homogenization of the liquid culture by several syringe passages through a thin needle ("mini-French press"). The yellow colonies taken into liquid medium with Hyl resulted in positive cultures one of which was designated strain AB-hyl4. The primary analysis of culture purity was checked microscopically, by Sanger sequencing of the 16S rRNA gene and by the genome analysis.

Microscopy and chemotaxonomy

Phase contrast microscopy (Zeiss Axioplan Imaging 2 microscope, Göttingen, Germany) was applied for routine checks and electron microscopy - to examine flagellation and cell ultrastructural organization. For the latter, the cells were centrifuged, resuspended in 0.5 M NaCl and fixed with *p*-formaldehyde (final concentration 3 %, *v*/v) at room temperature for 2 h, then washed again with the same NaCl solution. For whole cell imaging, the fixed cells were positively contrasted with 1 % (*w*/*v*) uranyl acetate. For thin sectioning, additional fixation was done by 1 % (*w*/w) OsO_4 and the obtained sections were poststained in lead citrate and uranyl acetate (1 % each) (Reynolds, 1963). The preparations were examined with a Jeol JEM-1400 electron microscope (Japan).

Membrane polar lipids and respiratory quinones were extracted with a modified Bligh-Dyer procedure from freeze-dried cells grown at 30 °C at 0.6 M total Na^+, pH 9.5 with Hyl until the late exponential growth phase and analyzed by Ultra High Pressure Liquid Chromatography-High Resolution Mass Spectrometry (UHPLC-HRMS^n), as described previously (Bale et al., 2021). For the core fatty acids profiling, the cells were hydrolyzed in HCl/MeOH (1.5 N) and extracted with dichloromethane and further processed, analyzed and lipids identified as described by Bale et al. (2019).

Growth physiology

Salinity tolerance was examined in the sodium carbonate/bicarbonate buffer with a pH of 9.5 within the total Na^+ range from 0.2 to 2.5 M. The basic media also contained 0.1 M NaCl and 1 g l^{-1} of K_2HPO_4. After sterilization, the media were supplemented with 1 ml/l of acidic trace metal and filter-sterilized vitamin mix solutions (Pfennig and Lippert, 1966) and 1 mM Mg sulfate from 1 M stock solution. The standard incubation temperature was 30 °C on o rotary shaker at 150 rpm (except for anaerobic tests). The growth pH range was studied using 50 mM HEPES/50 mM K-P/0.6 M NaCl for the neutral range from 6 to 8, 0.6 M bicarbonate/NaCl for the intermediate pH 8–8.5 and bicarbonate/carbonate with 0.6 M total Na^+ for the alkaline range from pH 8.5–10.5. The pH values measured at the end of experiments were considered to be the actual values. Because of highly aggregated biomass, the growth intensity was quantified by measuring cell protein (Lowry et al., 1951) after syringe-pressurized homogenization of the cultures. All other growth tests (temperature range, substrate utilization profiling, anaerobic growth) were done in carbonate medium with 0.6 M total Na^+ and pH 9.5. Anoxic medium was prepared using a sterile argon gas flushing-cold boiling evacuation system (3 cycles) in 23 ml serum bottles with 10 ml medium closed with butyl rubber stoppers. The medium was made anaerobic by final addition of 0.2 mM of sterile Na_2S.

Genome sequencing, phylogenomic analysis and functional genomics

Genomic DNA was extracted with the FastDNA™ SPIN Kit for Soil (MP Biomedicals, United States). A shotgun WGS library preparation and sequencing were performed using Illumina DNA Prep (M) Tagmentation kit and NovaSeq 6000 (2 × 151 bp) system (Illumina, San Diego, CA, USA). The genomes were assembled with Unicycler v.0.5.0 (Wick et al., 2017) and submitted for automatic annotation to the PGAP (Tatusova et al., 2016) in GenBank. The draft genome statistics of strain AB-hyl4 and of the two most closely related MAGs from the same habitat are shown in Supplementary **Table S1**.

For phylogenomic reconstructions, 120 single copy conserved bacterial marker proteins were used according to the Genome Taxonomy Database (Rinke et al., 2021), aligned using GTDB-Tk v2.4.0 (Chaumeil et al., 2022) and trimmed by trimAl 2.0 using "-automated1" and "-gt 0.93" modes (Capella-Gutiérrez et al., 2009) resulting in 22,151 aa length alignment. The trees were built with the IQ-TREE2 program v2.2.0.3 (Minh et al., 2020) with fast model selection via ModelFinder (Kalyaanamoorthy et al., 2017) and ultrafast bootstrap approximation (Minh et al., 2013) as well as approximate likelihood-ratio test for branches (Anisimova and Gascuel, 2006). The whole genome comparison included Average Nucleotide Identity (ANI), using Pyani 0.2.12 (Pritchard et al., 2016) and Average Amino acid Identity (AAI) by the EzAAI v1.1 (Kim et al., 2021).

To assess the possible presence and relative abundance of AB-hyl4-related microorganisms in publicly available metagenomes, we performed read recruitment analysis. The metagenomes were downloaded from the Sequencing Reads Archive (SRA) and the relative coverage of the AB-hyl4 genome compared to other MAGs of each specific metagenome was calculated using the MetaWRAP "quant_bins" workflow (Uritskiy et al., 2018). A search among high-throughput sequencing data for 16S rRNA gene regions was performed by IMNGS (Lagkouvardos et al., 2016) using 95 % similarity threshold and 200 bp as a minimum

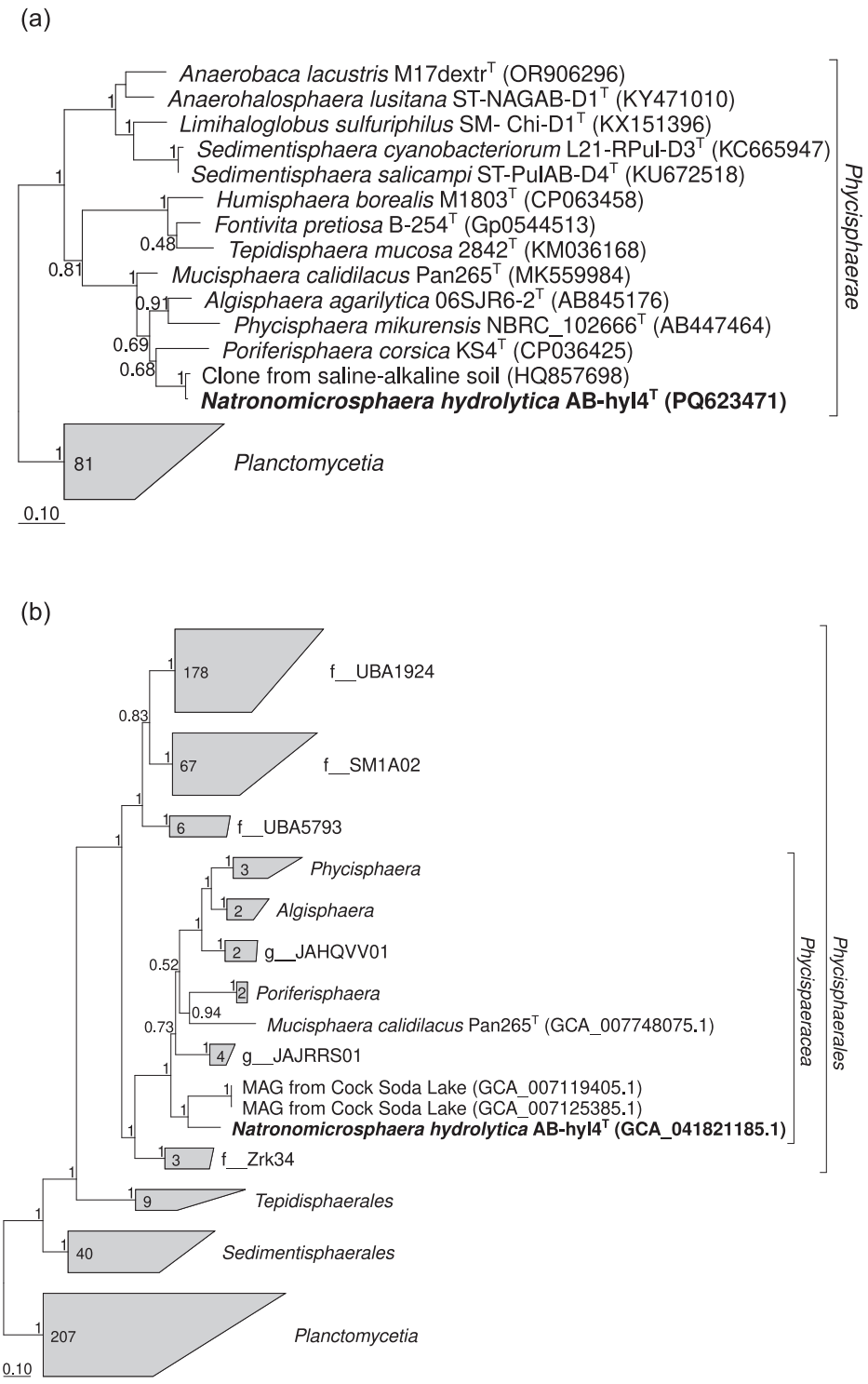

Fig. 1. Phylogenetic placement of strain AB-hyl4 within the order *Phycisphaerales* based on (**a**) 16S rRNA gene sequences and (**b**) concatenated amino acid sequences of 120 bacterial single copy conserved marker proteins with taxonomic designations according to the Genome Taxonomy DataBase (the length of the alignment is 22,151 aa). Bootstrap consensus tree is shown with values placed at the nodes. Bar, 0.1 change per position.

size threshold.

Identification of hyaluronidase PL8-GH88 genes was performed by the NCBI Blastp program (Altschul et al., 1997) against the CAZy database (Drula et al., 2022). Arrangement of gene sequences and manual gene annotation was performed by Geneious Prime 2025 (Dotmatics Inc). The automated annotation of carbohydrate-active enzyme and substrate (dbCAN3) (Zheng et al., 2023) was applied to the AB-hyl4 genome along with Signal 6.0 server (Teufel et al., 2022) to predict the presence of signal peptides and the location of their cleavage sites.

Results and discussion

Phylogenetic analysis, classification and distribution

The 16S rRNA gene sequence analysis placed strain AB-hyl4 into the family *Phycisphaeraceae* within the phylum *Planctomycetota* as a deep

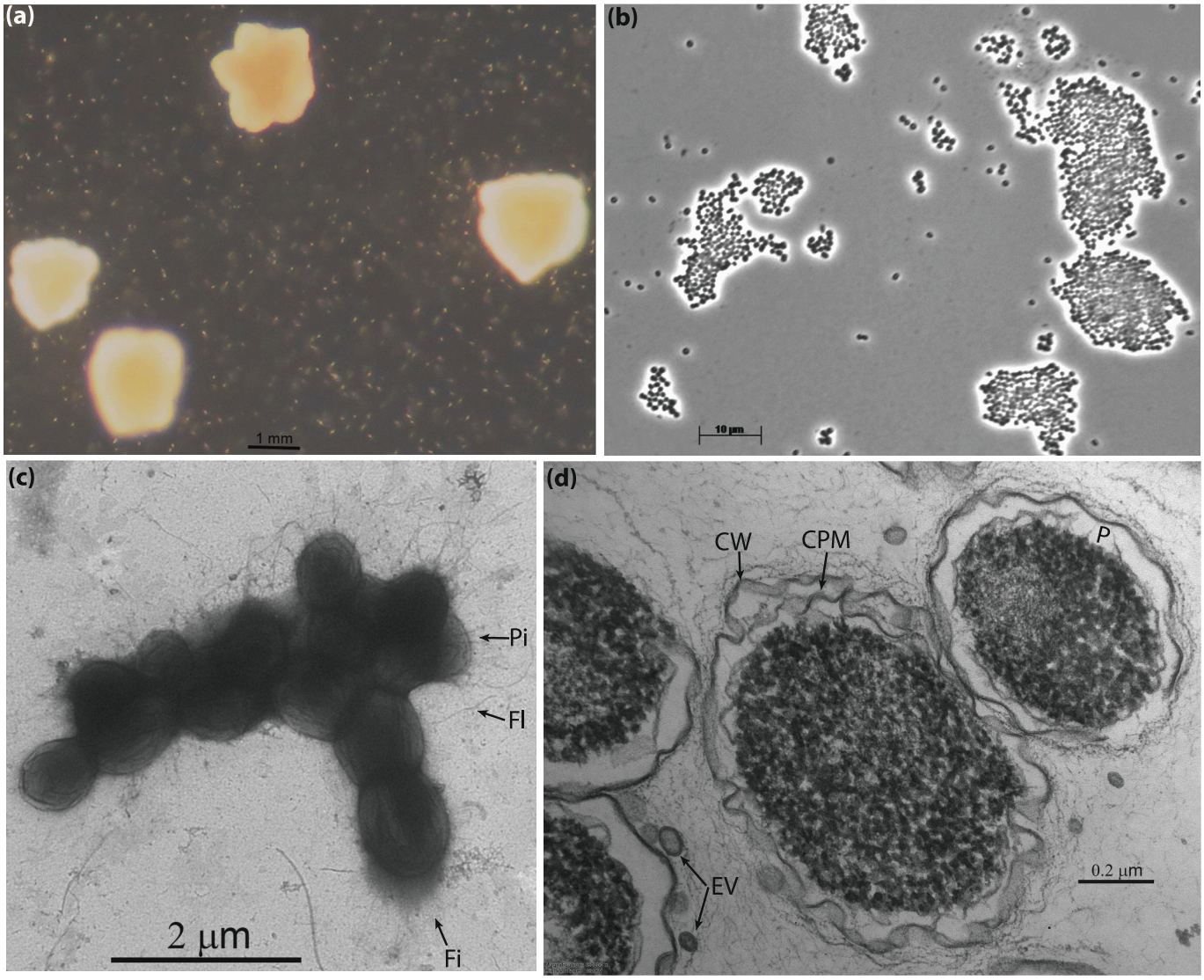

Fig. 2. Colonies (inside soft agar) (**a**), and cell morphology (**b-d**) of strain AB-hyl4 grown with HMW hyaluronate at 0.6 M total Na^+, pH 9.5 and 30 °C. (**b**), phase contrast microphotograph; (**c**), transmission electron microscopy microphotograph showing flagellation and surface appendages (pili or fimbria); (**d**), thin section electron microscopy microphotograph showing Gram-negative type of surface ultrastructure with an extended periplasm (**P**) and highly fragmented/segregated cytoplasm. **CW**, cell wall; **CPM** – cytoplasmic membrane; **EV**, extracellular vesicles; **Fl**, flagellum; **Pi**, pili-like; **Fi**, fimbria-like.

independent lineage (Fig. 1a). Hence, it represents the first isolated pure culture of this phylum obtained from soda lakes. Its 16S rRNA gene differs substantially from other representatives of the family: from 87.4 % identity with *Phycisphaera mikurensis* FYK2301M01^T to 89.81 % with *Mucisphaera calidilacus* Pan265^T. Among 42,707 sequences of the 16S rRNA gene belonging to the class *Phycisphaerae* in the SILVA 138.2 database (Quast et al., 2013), only one was closely related to the AB-hyl4 - HQ857698 (98.58 % identity) belonging to a clone from a saline-alkaline soil in China. Among the publicly available data from high-throughput sequencing of 16S rRNA gene regions, we found several studies where some phylotypes were found to be at least 99 % identical to the AB-hyl4. In these works, saline-alkaline soils from Songnen Plain (BioProject PRJNA509045, PRJNA503757) and samples from Qinghai-Tibetan saline lakes (PRJNA280140) were analyzed. In all cases, the abundance of these bacteria was in the range of 0.04–0.2 %.

Phylogenetic reconstruction based on 120 bacterial conserved protein markers (Parks et al., 2018) confirmed assignment of strain AB-hyl4 into *Phycispaeraceae* and placed it as a separate genus-level lineage (Fig. 1**b**). This phylogenetic lineage is designated in the GTDB release RS220 as SKPT01 and includes two closely related MAGs. These MAGs were assembled from surface sediments of Cock Soda Lake, a moderately saline soda lake in the Kulunda Steppe (Vavourakis et al., 2019), and represent another species of the same genus as the AB-hyl4: 86.2 % of ANI and 63.8 % of AAI between the genomes of AB-hyl4 and MAG GCA_007119405.

To assess the representation of this new genus in natural ecosystems, we analyzed four metagenomes from Cock Soda Lake in Kulunda Steppe (BioProject PRJNA453733), which is in the same region from which AB-hyl4 was isolated. The estimated relative content of the MAGs closely related to AB-hyl4 in the top 2–5 cm oxic sediment layer was around 0.02 %, i.e. they represented an extremely minor part of the community. Whereas the MAG GCA_007119405, probably representing another species of the genus detected only in the top 2 cm sediment layer had a much higher relative abundance of 0.13–0.16 %.

Cell morphology and chemotaxonomy

AB-hyl4 formed hard yellowish colonies inside soft agar (Fig. 2 **a**). The cells, both in colonies and in liquid cultures, are mostly present in large aggregates (Fig. 2 **b**). They are small cocci-ovoids, from 0.5 to 1 µm

Table 1
Lipid composition of strain ABhyl4 (the major components are in bold; species with a relative abundance <0.5 % are not listed).

Component	Relative abundance (%)
Polar lipid-derived fatty acids	
C14:1ω12	0.8
*anteiso*C15:0	0.5
*iso*C16:0	**24.9**
C16:1ω7	0.9
$C_{16:0}$	**10.7**
*anteiso*C17:0	**13.1**
C17:0	0.5
C18:1ω9	**18.1**
C18:0	**10.7**
C20:0	0.5
29-OH C30:0	3.3
Sum of the other OH-FA*	1.3
Neutral lipids	
Sum of C17:1 hydrocarbons	**6.1**
Sum of C19:1 hydrocarbons	3.2
Bacteriohopanetetrol	3.9

3-OH C20:0; 27-OH C28:0; 31-OH C32:0.
* includes: *iso* 3-OH C14:0; *iso*-3-OH C16:0; *anteiso*-3-OH C15:0; 3-OH C18:0;

in diameter, actively motile by several flagella and also have other short surface filaments, probably either pili or fimbria (Fig. 2 **c**). Thin sectioning showed a typical Gram-negative cell ultrastructure but with several unusual features (Fig. 2 **d**): 1 – an overlarge periplasm; 2 – a presence of extracellular (but still cell-associated) membrane vesicles; 3 – a complete fragmentation of cytoplasm into protein-rich irregular coccoid structures with an average diameter of 20 nm. We can only speculate that those might represent Bacterial Micro Compartments (BMC) (Kennedy et al., 2021; Kerfeld et al., 2018), which genomic locus can be clearly identified in AB-hyl4, as well as in the two related genera in *Phycisphaeraceae* (see below).

The only respiratory quinone identified in strain AB-hyl4 was MK-6. The dominant identified membrane phospholipids were phosphatidylcholines (PC). There exists no information on the composition of membrane polar lipids in other known genera of the family *Phycisphaeracea*. The dominant polar lipid fatty acids were *iso*C16:0, C16:0, *anteiso*-C17:0, C18:1ω9 and C18:0 (**Table 1**), with a range of other fatty acids and long-chain hydroxy fatty acids in lower abundance. While this fatty acid distribution is different from those detected in two related genera of the family *Phycisphaeraceae,* it was not uncommon in other planctomycetes, in particular the presence of the long-chain hydroxy fatty acids (Kulichevskaya et al., 2017). Additionally, a series of monounsaturated hydrocarbons were detected, ranging in length between C17 and C21 (**Table 1**), as well as hopanoids. The presence of hopanoids in members of *Planctomycetota* has been shown before (Sinninghe Damsté et al., 2004). Hopanoids are considered to be analogous to sterols in function, i.e. increasing cytoplasmic membrane rigidity. They and the other types of neutral lipids might also function as an additional barrier for the proton leakage in alkaliphiles (Haines, 2001).

Growth physiology

Strain AB-hyl4 is an obligately aerobic organoheterotroph with a very narrow substrate spectrum for growth limited to Hyl polymer (optimal growth), chondroitin sulfate (sulfated heteropolymer of *N*-acetylgalactosamine and glucuronic acid) and the trisaccharide melizitose (moderate growth) and glycerol (weak growth). During growth on all these substrates cells were highly aggregated. The following polysaccharide were tested negative as substrates: agarose, alginate, heparin sulfate, pectin (citrus or apple), polygalacturonate, rhamnogalacturonan, starch, dextran, beech xylan, amorphous chitin and cellulose, xyloglucan, beta-mannan. The monosugars, alcohols and organic acids tested but not utilized included glucose, fructose, arabinose, galactose, mannose, rhamnose, raffinose, trehalose, fucose, lyxose, xylose, lactose, ribose, sucrose, cellobiose, maltose, melibiose, glucosamine, *N*-acetylglucosamine; mannitol, arabinol; acetate, propionate, pyruvate, lactate, succinate, fumarate. Tests for anaerobic fermentative growth and anaerobic respiration with sulfur or 2 mM nitrite (see below) with Hyl or glycerol as substrates were also negative. Ammonium and urea supported growth of AB-hyl4 as the N-source in presence of all utilized carbon substrates, while nitrate did not.

Salt (as sodium carbonates) and pH (at 0.6 M total Na^+) profiling (Fig. 3) characterized the new isolate as a moderately salt-tolerant obligate alkaliphile with a salinity range for growth on Hyl from 0.3 to 2.0 M total Na^+ (optimum at 0.4–0.6 M) and the (actual measured) pH from 8.2 to 10.2 (optimum at 9.0–9.3). At pH 9.0 and 0.6 M total Na^+ AB-hyl4 grew between 20 and 40 °C (optimum at 30 °C). A phenotypic comparison of AB-hyl4 and four genera from the family *Phycisphaeraceae* is presented in Table 2.

Functional genome analysis

Hyaluronic acid utilizing potential

The key functional property of strain AB-hyl4 is to utilize Hyl, a linear polysaccharide composed of repeating disaccharide units of [(1➔3) β-D-*N*-acetyl-glucosamine-(1➔4) β-D-glucuronic acid] as growth substrate. Along with chondroitin sulfate, dermatan sulfate, heparin/heparan sulfate, and keratan sulfate, Hyl belongs to the group of acidic glycosaminoglycans (GAG), previously called mucopolysaccharides. All of these linear polymers are composed of core disaccharide units formed

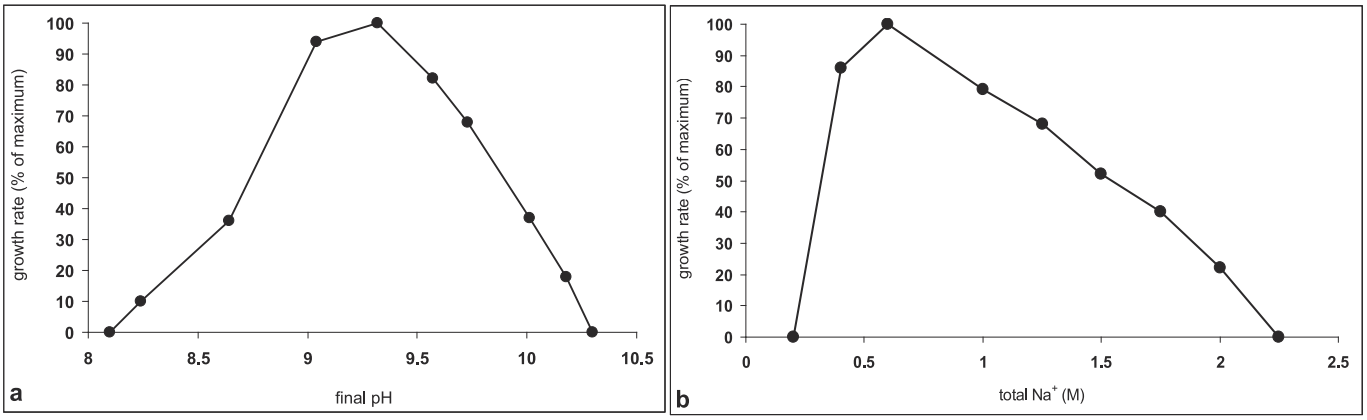

Fig. 3. pH (at 0.6 M Na^+) and salinity as sodium carbonates (at pH 9.5) for growth of strain AB-hyl4 with HMW Hyl at 30 °C. The biomass was estimated by measuring cell protein (average values from a duplicate experiment).

Table 2
Properties of strain AB-hyl4 comparative to its closest related genera withing the family *Phycisphaeraceae*.

Property	**AB-hyl4**	*Poriferisphaera*[a]	*Mucisphaera*[b]	*Algisphaera*[c]	*Phycisphaera*[d]
Morphological features					
Cell shape	motile aggregated cocci	nonmotile cocci	motile cocci	motile cocci	motile cocci
Cell diameter (μm)	0.5–1.0	0.4–0.8	0.4–1.1	1.0–1.2	0.5–1.3
Pili/fimbria-like	+	+	+	–	+
Intracellular membranes	–	nr	nr	–	+
Extracellular membrane vesicles	+	+	nr	–	–
Cell wall peptidoglycan	+ (genomic evidence)	+ (genomic evidence)	+ (genomic evidence)	– (chemical analysis) + (genomic evidence)	– (chemical analysis) + (genomic evidence)
BMC	+ (genomic evidence)	+ (genomic evidence)	+ (genomic evidence)	–	–
Cell pigmentation	+ yellow	–	+ pink	+ pink	+ pink
Relation to oxygen	obligate aerobe	obligate aerobe	obligate aerobe	obligate aerobe	facultative anaerobe
Growth substrates					
polysaccharides	hyaluronan; chondroitin	nr	nr	alginate, agar, starch	agar, glycogen (v)
sugars	milezitose, glycerol	*N*-acetylglucosamine*	*N*-acetylglucosamine*	cellobiose	arabinose, glucose, fructose, cellobiose (v), maltose (v), mannose (v), rhamnose (v), xylose (fermentation)
urea as *N*-source	+ (growth) + (urease genomic locus)	– (genomic evidence)	– (genomic evidence)	+(urease activity) + (urease genomic locus)	– (urease activity) + (urease genomic locus)
Salinity range (opt.) M	0.3-2.0 (0.4-0.6) total Na^+	0-0.7 (0) NaCl/sea water	nr	up to 1.0 NaCl	0.2-1.0 (0.5) NaCl/sea water
pH range (opt.)	8.2–10.2 (9.0-9.3)**	6.5–8.0 (7.5)	5.5–8.5 (7-8)	6.0–8.0 (7.0)	nr (neutraphilic)
Max. temperature (°C)	40	30	36	30	30
Intact membrane polar lipids		nr	nr	nr	nr
Predominant polar lipid fatty acids	*i*C16:0, C16:0, *ai*C17:0, C18:1ω9, C18:0	nr	nr	*ai*C15:0, C16:0, C18:1ω9c, C15:0	C16:0, *i*-C16:0, *i*C16:1, 3-OH *i*-C14
Respiratory lipoquinones	MK-6	nr	nr	MK-6	MK-6
Genome size (Mbp)	4.6	4.3	3.5	4.2	3.9
G + C (%, whole genome)	62.5	48.7	63.9	63	73
Habitat	soda lakes			marine	

nr, not reported; (v), variable in different strains; BMC – biological microcompartments; *- enrichment and isolation substrate (no other substrates were reported); ** - final pH values.
a[Kallscheuer et al., 2020]; b[Kallscheuer et al., 2022]; c[Yoon et al., 2014]; d[Fukunaga et al., 2009].

by glucuronic or iduronic acid linked to an aminoglycan or amino sugar (*N*-acetylglucosamine or *N*-acetylgalactosamine) by α-1➔4, β-1➔3 or β-1➔4 glycosidic bonds. With the exception of Hyl, these high-molecular-weight GAGs frequently contain sulfate groups in amino sugar and/or uronate residues. As major components of extracellular matrices, GAGs are ubiquitously present in all tissues and organs of vertebrates, especially mammals, constituting various proteoglycans (PGs) that serve as physical scaffolds for cellular components, homeostasis, tissue formation and cell differentiation (Oiki et al., 2017). AB-hyl4 did not utilize the abovementioned GAGs, except for a weak growth on chondroitin sulfate. Such a high level of specialization of AB-hyl4, is rather puzzling and somewhat difficult to explain. Although Hyl is widely distributed in vertebrate epithelial, connective and neural tissues, it is virtually not synthesized by either invertebrates or unicellular microorganisms (Yasuda, 2011; Senni et al., 2011). Since the haloalkaline lakes from which AB-hyl4 was isolated are devoid of any vertebrate inhabitants, except perhaps only the migratory birds such as waders that feed on brine shrimp and occasional animal carcass that has accidentally ended up in the lake, it is unlikely that Hyl is present in sufficient quantities to be any significant component of the ecosystem food web.

Consistent with the relatively limited catabolic potential towards various carbohydrates, the Ab-hyl4 genome contains a scant set of Carbohydrate-Active Enzyme (CAZymes) genes, involved in breakup of glycosidic bonds in polysaccharides and glycoproteins; only five polysaccharide lyases, belonging to four different families, were identified (Supplementary **Table S2**). Since Hyl typically is present in the extracellular matrix as a large molecule of about 3–7 MDa, its primary degradation pathway must involve an extracellular (endo)hydrolytic step mediated by polysaccharide lyases and/or glycosyl hydrolases. Extracellularly secreted proteins typically possess a signal peptide. On basis of this characteristic, one of the five polysaccharide lyases was identified as a putative hyaluronate lyase (NhHAase) (Supplementary **Table S2**).

The open reading frame of this lyase (locus tag ACERK3_13535, accession number MFA9479308) was 2936 bp in length, and the deduced protein, consisting of 978 amino acid residues, had a theoretical Mw and *pI* of 111.5 kDa and 4.50, respectively. According to SignalP 6.0, NhHAase had a Sec/SPI type signal peptide of 27 amino acids at its N-terminus and the theoretical Mw and *pI* of mature lyase were 108.6 kDa and 4.44, respectively. An NCBI conservative domains (CD) search revealed that NhHAase contained N-terminal Lyase_N module (Val^{42}-Ala^{195}) predominantly found in chondroitin ABC lyase I and hyaluronate lyase, both of which belong to the GAG polysaccharide lyase (PL) 8 family, required for binding of the protein to long glycosaminoglycan chains. Correspondingly to this type of lyases, NhHAase possessed a catalytic Lyase_8 (Lys^{216}-Leu^{545}) and a GAG-lyase superfamily (Met^{295}-Pro^{910}) modules.

According to the CAZy classification database (Lombard et al., 2014), the PL8 family currently consists of four subfamilies of secreted bacterial lyases capable of cleaving acidic polysaccharides containing 1,4-β-D-hexosaminyl and 1,3-β-D-glucoronosyl or 1,3-a-L-iduronosyl linkages, which are classified as hyaluronic acid or hyaluronan and chondroitin. Typically for this family of GAG-degrading lyases, depolymerization occurs via exolytic β-elimination mechanism, resulting in the formation of unsaturated GAG disaccharides with a C=C double bond at the non-reducing termini (Li and Jedrzejas, 2001; Stern and Jedrzejas, 2006; Jedrzejas, 2007). Based on the phylogenetic tree constructed for the GAG-lyase catalytic modules of the PL8 lyase family from the NCBI database, NhHAase showed <36 % identity with any of the known lyases from cultured organisms. It was somewhat clustered among the members of PL8 subfamily 2, which was further confirmed by taking into account the domain architecture of the analyzed lyases (Fig. 4). Only members of this subfamily possess an N-terminal domain belonging to the pfam09092 protein family, predominantly found in type I chondroitin ABC lyases (EC 4.2.2.4). This domain is required for protein binding to long chain glycosaminoglycans (Huang et al., 2003). However, such a distant position suggests that, together with a number

of enzymes annotated from metagenome-assembled genomes belonging to various members of the PVC superphylum and the *Armatimonadota* phylum, it may belong to a new branch of the PL8 family. However, such a distant position suggests that, together with a number of enzymes annotated from metagenome-assembled genomes belonging to various members of the PVC superphylum and the *Armatimonadota* phylum, it may belong to a new branch of the PL8 family. However, such a distant position suggests that, together with a number of enzymes annotated

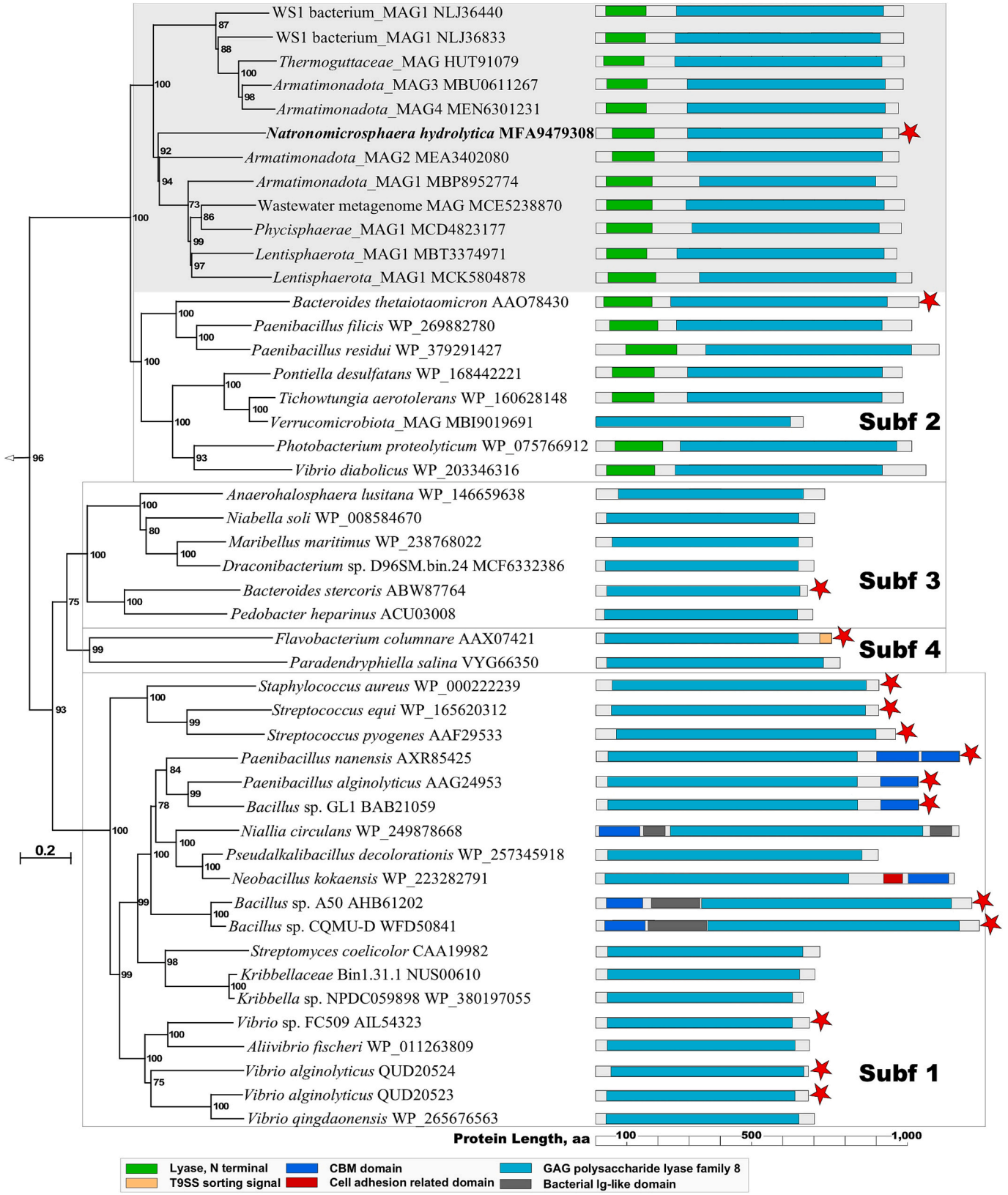

(caption on next page)

Fig. 4. Maximum Likelihood phylogenetic tree placing NhHAase among hyaluronate lyases and other enzymes of the PL8 family retrieved from GenBank. Only catalytic GAG-lyase modules were considered in the phylogenetic analysis. Totally 47 sequences belonging to all four PL8 subfamilies were taken for the analysis. The phylogenetic tree was generated using MEGA-X (Kumar et al., 2018) and the tree with the highest log-likelihood is shown. Hyaluronate lyase (NhHAase) from AB-hyl4 and the cluster of predicted NhHAase-related enzymes are highlighted in bold and gray color, respectively. Bootstrap values (1000 replicates) are shown next to the branches. The tree was rooted with PL22 family oligogalacturonate lyase WP_238817456. The bar represents 0.2 amino acid substitutions per site. The architectural structure and length of the corresponding fragments of PL8 polysaccharide lyases are presented based on protein domains identified using InterPro prediction (Mitchell et al., 2019) and NCBI conserved domain search (Marchler-Bauer et al., 2017; Wang et al., 2023). The catalytic domains of glycosaminoglycan (GAG) polysaccharide lyase are shown in light blue, while the identity of all other domains is indicated by different colors in the figure. Abbreviations are as follows: CBM, carbohydrate binding module; T9SS, type IX secretion system sorting signals; Ig-like, immunoglobulin-like domain. PL8 family lyases from bacteria that have been experimentally shown to grow and degrade various glycosaminoglycans, including hyaluronate and chondroitin are indicated by asterisks. (For interpretation of the references to color in this figure legend, the reader is referred to the web version of this article.)

from metagenome-assembled genomes belonging to various members of the PVC superphylum and the *Armatimonadota* phylum, it may belong to a new branch of the PL8 family.

As mentioned above, AB-hyl4 has an ability, although weak, to grow on chondroitin sulfate (CS) as the only carbon and energy source. It is formed of repeating disaccharide units composed of D-glucuronic acid and *N*-acetyl-D-galactosamine, $[GlcA\text{-}\beta(1,3)\text{-}GalNAc\text{-}\beta(1,4)]_n$, O4 or O6 sulfation (Benito-Arenas et al., 2019). Hyl is similar to chondroitin but replaces GalNAc with *N*-acetyl-D-glucosamine (GlcNAc) and contains no sulfation. The extracellular polysaccharide lyase PL8 (ACERK3_13535) resembles typical features of hyaluronidases (HAase) of PL8 family, which generally have lower activity towards chondroitin sulfate due to its modifications (Wang et al., 2017). Many bacterial hyaluronidases digest Hyl via initial non-progressive endolytic activity, followed by exolytic degradation with the generation of unsaturated disaccharides as final products (Hovingh and Linker, 1999; Jedrzejas et al., 2002). However, the digestion of CS by these lyases is only via an endolytic action leading to formation of sulfated oligosaccharides (Wang et al., 2017). Considering this fact, we searched for genes specifically involved in metabolism of chondroitin, such as sulfo-acetylhexosaminidases and sulfohydrolases. Among those, special attention was given to sequences possessing a signal peptide, suggesting that these enzymes are either extracellular or surface-localized. Twelve of such predicted proteins were identified with a catalytic N-terminal distantly related to the *endo*-hexosaminidases of the glycosyl hydrolases family GH20 (Supplementary **Table S1**). Some of them additionally harbor a C-terminal sugar binding domain of the GH2 family. Recent studies characterized such proteins as members of new GH163 and GH185 families of 6-sulfo-*N*-acetylhexoseaminidases (Armstrong et al., 2017; Higgins et al., 2021; Bains et al., 2023). Furthermore, the AB-hyl4 genome contains seven genes for predicted sulfatases, among which only one, ACERK3_06510 (MFA9477948), was annotated as *N*-sulfoglucosamine sulfohydrolase (SGSH). The sequence lacked a signal peptide suggesting that this enzyme is localized within the cytoplasm and act on imported disaccharides.

Import and utilization of Hyl metabolites by AB-hyl4 as predicted from genome analysis and cultivation.

The subsequent metabolic pathway of Hyl, initiated by the primary hydrolytic lyases, such as PL8, has been well studied in Hyl-utilizing bacteria (Hashimoto et al., 1999; Itoh et al., 2006; Oiki et al., 2017; Wang et al., 2021, 2022). The resulting unsaturated disaccharide is cleaved in the cytoplasm into their constituent monosaccharides, Δ4,5GlcUA and GlcNAc, by unsaturated glucuronyl hydrolase (UGL) via hydration of the C=C double bonds. According to the CAZy database, all known UGLs are solely members of the glycosyl hydrolase (GH) family GH88 (Lombard et al., 2014). As shown earlier (Maruyama et al., 2015; Wang et al., 2021, Wang et al., 2023), unsaturated glucuronate is further metabolized into pyruvate and glyceraldehyde-3-phosphate via subsequent reactions of the corresponding isomerase (KduI), NADH-dependent hydrogenase (KduD), kinase (KdgK), and aldolase (KdgA). The complete set of genes for this pathway of Hyl degradation and following assimilation of Δ4,5-glucuronate was identified in the AB-hyl4 genome (**Table 3**). As for GlcNAc metabolism, in AB-hyl4 it resembles the reverse variant of the hexose biosynthesis pathway (Chen and

Table 3
Key functional proteins involved in transport and metabolism of hyaluronan encoded in the genome of strain AB-hyl4.

GCA-tags	Protein	Putative function
	Transport	
MFA9477340	ExbD/TolR family protein	TonB-dependent transport system
MFA9477341	ExbD/TolR family protein	
MFA9477342	MotA/TolQ/ExbB proton channel family protein	
MFA9480140	TonB-dependent receptor family protein	
MFA9480141	Putative ATPase	
MFA9480142	MotA/TolQ/ExbB proton channel family protein	
MFA9480143	MotA/TolQ/ExbB proton channel family protein	
MFA9480144	ExbD/TolR family protein	
MFA9480145	TonB family protein	
MFA9477140	phosphoenolpyruvate-protein phosphotransferase	PTS-phosphoenolpyruvate-dependent sugar phosphotransferase system
MFA9477235	PTS sugar transporter subunit EIIA_1	
MFA9477236	HPr family phosphocarrier protein	
MFA9479597	PTS sugar transporter subunit EIIA_2	
MFA9477367	ABC transporter permease	Carbohydrate ATPase-coupled transmembrane transporter activity (ABC transporters)
MFA9477368	ABC transporter family permease subunit	
MFA9477369	ABC transporter ATP-binding protein	
MFA9477370	ABC transporter solute-binding protein	
MFA9477822	carbohydrate ABC transporter permease	
MFA9477823	sugar-binding protein	
MFA9478109	ABC transporter multiple sugar permease subunit	
MFA9478110	sugar-binding protein	
	Hyaluronan metabolism	
MFA9479308	chondroitinase family polysaccharide lyase	Hyaluronan depolymerization
MFA9480320	Unsaturated glucuronyl hydrolase	Disaccharide hydrolysis
MFA9478286	glucuronate isomerase, KduI	D-glucuronate metabolism
MFA9480321	2-dehydro-3-deoxy-D-gluconate 5-dehydrogenase KduD	
MFA9479802	D-gluconate kinase KdgK	
MFA9477880	2-dehydro-3-deoxy-phosphogluconate aldolase KdgA	
MFA9477624	1-phosphofructokinase family hexose kinase HK	
MFA9477708	*N*-acetylglucosamine-6-phosphate deacetylase NagA	GlcNAc metabolism
MFA9479200	*N*-acetylglucosamine-6-phosphate deacetylase NagA	
MFA9477667	glucosamine-6-phosphate deaminase NagB	

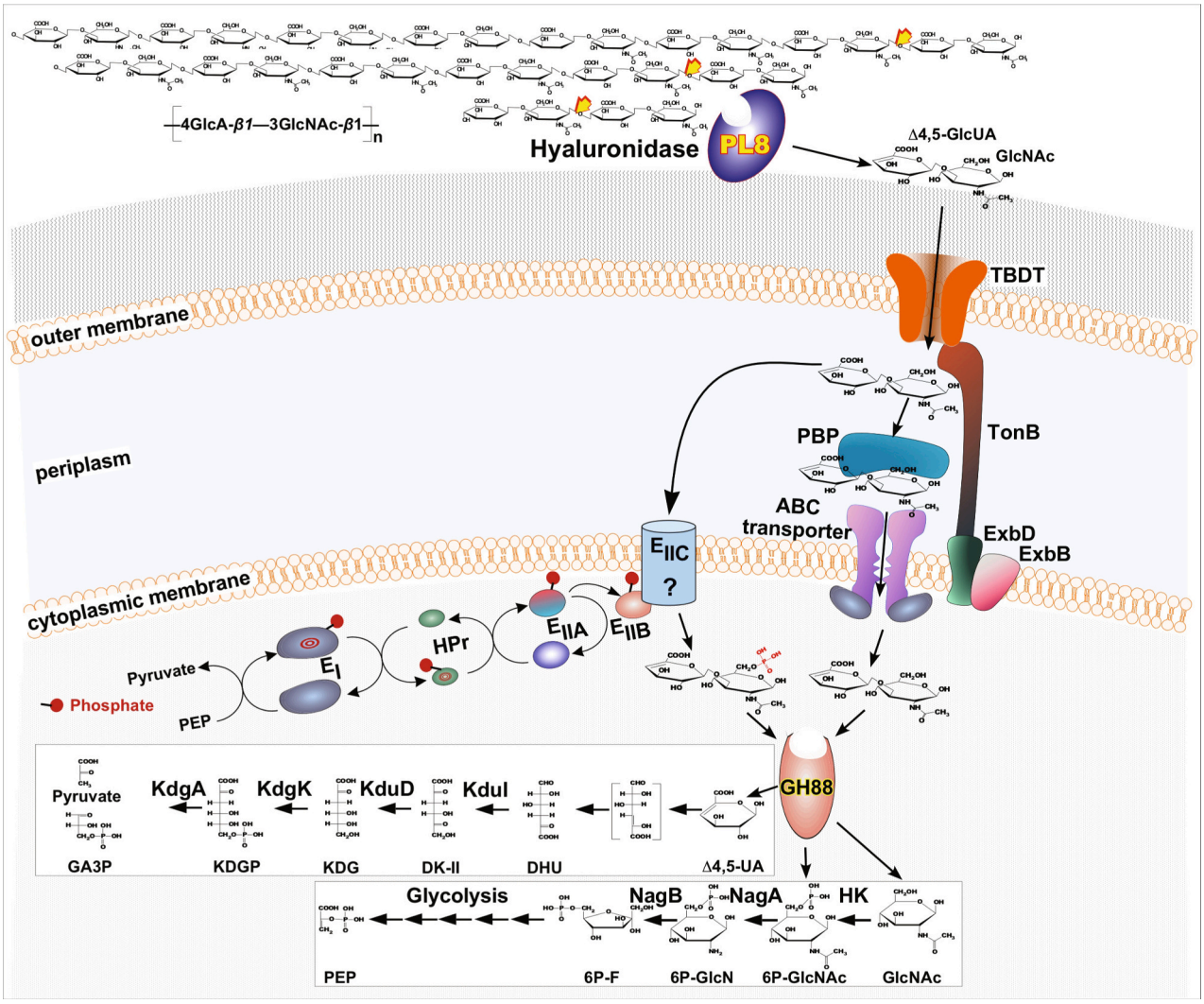

Fig. 5. Molecular mechanism of hyaluronan degradation by strain AB-hyl4. The extracellular polysaccharide lyase PL8 cleaves Hyl to produce unsaturated disaccharides, which are bound and transported into periplasm by TonB-dependent transport systems. The oligomers are further imported via the inner membrane into the cytoplasm by either the PTS system or the carbohydrate ABC transporters. The GH88 hydrolase processes disaccharides to Δ4,5GlcUA (unsaturated glucuronate) and GlcNAc (*N*-acetyl-D-glucosamine), which are further converted into pyruvate, glyceraldehyde-3-phosphate (GA3P) and phosphoenolpyruvate (PEP) by subsequent reactions of KduI isomerase>KduD reductase>KdgK kinase>KdgA aldolase>HK hexose kinase>NagA deacetylase >NagB deaminase. Transport enzyme abbreviation used: TBDT, TonB-dependent transporter; TonB, TonB receptor, ExbB and ExbD, proton channel family proteins; PBP, periplasmic binding protein. PTS, a sugar transport system specific to bacteria, is composed of Enzyme I (EI), histidine-containing phosphor-carrier protein (HPr), and Enzyme II (EII) with heterosubunits (IIA, IIB, and IIC). Substrate abbreviation used: DHU, 4-deoxy_L-*threo*-5-hexosulose-uronate; DK-II, 3-deoxy-D-*glycero*-2,5-hexodiulosonate; KDG, 2-keto-3-deoxy-D-gluconate; KDGP, 2-keto-3-deoxy-6-phosphogluconate; 6P-GlcNAc, *N*-acetyl-D-glucosamine-6-phosphate; 6P-GlcN, D-glucosamine-6-phosphate; 6P—F, fructose-6-phosphate.

Cheng, 2024), which, via action of the corresponding hexokinase, deacetylase and deaminase, leads to the formation of fructose-6-phosphate, which subsequently enters in glycolysis (**Table 3** and Fig. 5).

Previous studies on various human gut, soil and marine GAG-degrading bacteria have indicated the typical presence in their genomes of genetic cluster(s), termed Polysaccharide Utilization Loci (PULs). Along with an array of surface glycan-binding proteins and CAZymes, they also encode proteins responsible for the degradation and metabolism of resulted oligo- and monosaccharides, which expression is under control of cytoplasmic transcriptional regulators that sense specific carbohydrate (Blanvillain et al., 2007; Oiki et al., 2017; Wang et al., 2021, 2022; Hameleers et al., 2024 for further references). Furthermore, various sugar-specific transport systems are also found in the PUL clusters. These include phosphotransferase system (PTS) and TonB-dependent transporters as a part of periplasmic ATP-binding cassette (ABC) transporters (Oiki et al., 2017; Wang et al., 2021, 2022; Hameleers et al., 2024). In fact, more than twenty sugars have been identified to be imported by PTS, except for the sugars with a modification at C-6 position (Barabote and Saier, 2005).

Unlike all known GAG-degrading bacteria, the genome of AB-hyl4 does not have any signs of PUL, and all genes involved in the depolymerization and further use of the Hyl metabolites are scattered throughout the genome (**Table 3**). With regard to intracellular import of unsaturated disaccharides, both PTS, two TBDT systems (TonB-dependent transporter) and several periplasmic binding protein-dependent ABC sugar transporters are present in the AB-hyl4 genome, which allows to propose a scenario of central metabolism of Hyl by AB-hyl4 (Fig. 5). We hypothesize that depolymerization of Hyl to unsaturated disaccharides occurred by an extracellular PL8 (ACERK3_13535). The resulting Δ4,5-GlcUA-1,3-β-GlcNAc disaccharides are further transported into periplasm using TBDT-mechanism, as it was described for several Gram-negative bacteria, including moderate halophiles (Dong et al., 2024; Oiki et al., 2017; Wang et al., 2021, 2022; Zhang et al., 2024), and further imported into cytoplasm by either PTS or periplasmic

Table 4
Proteins involved in haloalkaliphilkic adaptation, energy metabolism and structural functions encoded in the genome of strain AB-hyl4.

Locus tag (MFA94+)	Protein	Putative function
Osmoprotection		
77,243;77,248–77,249	Dipeptide ABC transporter	
7244	Glutamyl aminopeptidase M42	Biosynthesis and balancing of osmoprotectant
7245	*N*-acetylglutaminylglutamine synthetase	*N*-acetylglutaminylglutamine amide (NAGGA)
7246	*N*-acetylglutaminylglutamine amidotransferase	
7490	BetT	High affinity glycine betaine exporter
78,977–78,978	McsS	Mechanosensitive channel
pH-ion homeostasis		
79,670–79,678	MrpABCD1D2D3EFG	Multisubunite sodium:proton antiporter
80,179–80,185	MnhABCDEFG	Multisubunite sodium:proton antiporter
79,663–79,664	CPA2/KefB	Na^+/K^+: H^+ antiporter
79,716	CPA2	Na^+: H^+ antiporter
79,738	NhaP/CPA1	K^+: H^+ antiporter
79,522–79,523	TrkAH	Potassium uptake (K^+: H^+ symporter)
79,736; 79,928	CaCA	Ca^{2+}: Na^+ antiporter
77,187	ClcA	Cl^-: H^+ antiporter (chloride channel)
Primary sodium pumps		
76,698	HppA	Sodium-translocating pyrophosphatase
78,375–78,378	OadABG/BirA	Sodium translocating oxaloacetate decarboxylase
Respiratory chain		
76,672/77309–77,311/ 77,330–77,334/ 77740/ 79,951/80192/80420	NuoC/DEF/NMLKJ/B/I/A/H	NADH-menaquionone oxido-reductase
77,384–77,388	CtaAG/BD/C	Cytochrome c oxidase *caa*$_3$ (1)
77,389–77,390	PetAB/C	Menaquinone-cytochrome *c* reductase
77,579–77,583	CtaABCDG	Cytochrome c oxidase *caa*$_3$ (2)
77,585–77,590	ActABCDEF	Alternative complex III
77,190/78979–78,986/ 79,080	Atpε/αΔBCAIγ/β	H^+-translocating F1F0 ATP synthase
78,382–78,383	NrfAH	Dissimilatory ammonifying nitrite reductase
Structural elements		
79,780	L-fuculose phosphate aldolase FucA	
79,782	propionaldehyde dehydrogenase EutE/ PduP	Microcompartment (encapsulins) locus
79,787	acetate/propionate kinase EutQ/PduW	
79,781; 79,883; 79,785	EutN/CcmL microcompartment protein	
79,786; 79,788–79,789	EutM/CcmK/PduA microcompartment protein	
Type II-IV secretion pili/fimbria proteins		
76,726–76,736	GspDCEFGKJ/PilD1D2OM	Locus 1
76,832–834/76847–851	GspAEF/PilM1M2NO	Locus 2
76,904–76,908	GspEG/PilOMN	Locus 3
77,618–7619/ 80096–097	GspE/PilT	Locus 4; Locus 6
78,328–78,333	FimT-FimU/PilVX1X2/GspJ	Locus 5
78,882	PilA/FimA	Major pili/fimbrial biogenesis protein
79,515–79,521	PulK/FimT-FimU/PilD1D2/GspEFG1G2	Locus 7
Cell wall peptidoglycan biosynthesis		
77,217	MurJ	UDP-*N*-acetylglucosamine–*N*-acetylmuramyl-(pentapeptide) pyrophosphoryl-undecaprenol *N*-acetylglucosamine transferase
78,550	MurE	UDP-*N*-acetylmuramyl-tripeptide synthetase
78,551	MurF	UDP-*N*-acetylmuramoyl-tripeptide–D-alanyl-D-alanine ligase
78,552	MraY	phospho-*N*-acetylmuramoyl-pentapeptide-transferase
78,731	MurA	UDP-*N*-acetylglucosamine 1-carboxyvinyl-transferase
78,787	MurD	UDP-*N*-acetylmuramoyl-L-alanine–D-glutamate ligase
78,806	MurJ	murein biosynthesis membrane protein (lipid II flippase)
79,395	MurC	UDP-*N*-acetylmuramate–L-alanine ligase
79,690	MurB	UDP-*N*-acetylmuramate dehydrogenase
Lipids/carotenoids synthesis		
77,173	phytoene/squalene synthase HpnD	
77,174	squalene synthase HpnC	Neutral lipid squalene synthesis
78,807	hydroxysqualene dehydroxylase HpnE	
77,275	phytoene desaturase CtrP	Synthesis of xanthophylls
77,277	phytoene desaturase CtrL/CarC	

binding protein-dependent ABC transporter. In the case of PTS, substrates (unsaturated disaccharides) are phosphorylated at the C-6 position of GlcNAc across the cytoplasmic membrane. Unsaturated disaccharides are further degraded to constituent monosaccharides (unsaturated uronate and amino sugar) by GH88 (ACERK3_18775), and the monosaccharides, Δ4,5GlcUA and GlcNAc, are metabolized to pyruvate, glyceraldehyde-3-phosphate and phosphoenolpyruvate, respectively (Fig. 5).

Table 5
Description of *Natronomicrosphaera* gen. nov., and *Natronomicrosphaera hydrolytica* sp. nov.

Parameter	genus: *Natronimicrosphaera*	Species: *hydrolytica*
Order name		
Genus name	*Natronomicrosphaera*	
Species name		*Natronomicrosphaera hydrolytica*
Status	gen. nov.	sp. nov.
Type species of the genus	*Natronomicrosphaera hydrolytica*	yes
Description of a new taxon	Na.tro.no.mi.cro.sphae'ra [N.L. neut. n. *natron*, arbitrarily derived from the Arabic n. *natrun* or *natron*, soda; Gr. masc. Adj. *mikros*, small; Gr. fem. n. *sphaîra*, a ball, sphere; N.L. fem. n. *Nantronomicrosphaera,* soda-loving small coccus]. The genus includes moderately salt-tolerant and alkaliphilic aerobic heterotrophic bacteria specialized on utilization of acidic polysaccharides for growth. Currently it includes a single species. A member of the order *Phycisphaerales*, phylum *Planctomycetota*. The type species is *Natrono-microsphaera hydrolytic*a. Found in soda lakes.	*hydrolytica* [hy.dro.ly'ti.ca. Gr. neut. n. *hydor*, water; Gr. masc. Adj. *lytikos*, dissolving, splitting; N.L. fem. Adj. *hydrolytica*, (polymer) dissolving]. Cells are Gram-negative, coccoid, 0.5–1.0 μm, motile by several flagella and also have shorter pili/fimbria-like surface appendages. The colonies are hard, yellowish, up to 2 mm, forming inside soft agar. The polar phospholipids are dominated by phosphatidylcholine and phosphatidylethanol-amine with phosphatidylglycerol as a minor component. The polar lipid fatty acids are dominated by *i*17:0, *i*17:1ω9c, 18:1ω9, *i*19:1ω9c and 16:0. The only respiratory lipoquinone is MK-6. Has a genetic potential to synthesize dipeptide osmolyte *N*-acetyl-glutaminyl-glutamine amide (NAGGA), cell wall peptidoglycan and Bacterial Microcompartments (BMC). Strictly aerobic organoheterotrophs utilizing only four compounds as carbon and energy source: polysaccharides hyaluronic acid and chondroitin, trisaccharide melezitose and glycerol. Ammonium and urea serve as the nitrogen source. Moderately salt-tolerant with the total Na^+ range (in the form of sodium carbonates) from 0.3 to 2.0 M of (optimum at 0.4–0.6 M). Obligate alkaliphilic with a pH range for growth from 8.2 to 10.2 (optimum at 9.0–9.3). Mesophilic, with the upper temperature limit for growth (at optimal pH and salinity) at 40 °C. The G + C content of the genomic DNA is 62.5 % (whole genome). The type strain, AB-hyl4 (DSMZ 117994 = UQM 41914), was isolated from a mix sample of surface sediments and brines from soda lakes in Kulunda Steppe (Altai, Russia).
Type strain		AB-hyl4^T
Culture collection numbers		DSMZ 117994; UQM 41914
Genome status		Draft
GenBank genome assembly		GCA_041821185
Genome size (Mbp)		4.6
16S-rRNA gene accession number in the GenBank		PQ623471
Country of origine		Russian Federation
Region		Altai
Source of isolation		Surface sediments from soda lakes
Latitude		N52°06'/N51°37'/N51°40'
Longitude		E79°09'/E79°50'/ E79°54'
Sampling date		July 2022
pH of the sample		10–10.5
Salinity of the sample		50–150
Number of strains in study		1

Haloalkalphilic adaptation, energy generation and structural features

Search for the genes coding for biosynthesis of osmolytes most common in soda lake natronophilic bacteria (ectoine, glycine betaine and *N*ε-acetyl-β-lysine) in the AB-hyl4 genome yielded no results. However, *N*-acetylated amino acids compound – a dipeptide *N*-acetyl-glutaminylglutamine amide (NAGGA), first discovered in halotolerant *Pseudomonas* species (Sagota et al., 2010), seems to be a possibility. Similar to *Pseudomonas*, it is encoded by a locus containing a dipeptide ABC transporter>glutamyl aminopeptidase M42 and two genes coding for the NAGGA synthesis: *N*-acetylglutaminylglutamine synthetase and *N*-acetylglutaminylglutamine amidotransferase. In addition, external glycine betaine can be imported by a high-affinity BCC transporter BetT (**Table 4**). With respect to the alkaliphilic adaptation-ion homeostasis, AB-hyl4 has two multisubunit Na^+: H^+ antiporters MnhABCDEFG and MrpEFGBCD1D2D3, two copies of monosubunit Na^+: H^+ antiporters CPA2, a K^+: H^+ antiporter NhaP/CPA1 and a K^+: H^+ symporter TrkAH. Furthermore, unusual for aerobic alkaliphiles, genes for two primary sodium pumps were identified: a sodium-translocating pyrophosphatase HppA and a sodium-translocating oxaloacetate decarboxylase OadABG. The latter type, so far, has been found exclusively in anaerobic bacteria (Buckel, 2001).

Since direct chemical analysis of murein, the key component of the cell wall peptidoglycan, in some of the genera in *Phycisphaeraceae* produced negative results, we made a Blast search for the presence of murein synthesis genes in strain AB-hyl4 and four type species belonging to *Phycisphaeraceae* using homologues from the genome of *Haloanaerosphaera* (Pradel et al., 2020). The results were positive for all five genomes (the complete set of eight genes in each) indicating high probability that all cultured members of the family do have the ability to produce peptidoglycan. The negative attempts for its direct detection then might have several explanations: 1 – the very thin peptidoglycan layer (as, for example, is evident in AB-hyl4) in combination with high content of EPS in all such bacteria might make extraction inefficient; 2 –

the exact composition of murein in this particular group might differ from the known ones in other bacteria with the Gram-negative structure of the cell wall.

The genome of AB-hyl4 includes seven loci coding for the components of type II-type IV secretion systems including pili-fimbria formation. Those are also common in the genomes of other members of *Phycisphaeraceae* and its formation is often evident from electron microscopy.

A large genomic locus (nine genes) is present in the genome of AB-hyl4 encoding the formation of biological microcompartments (BMC) or encapsulins – formed to enclose toxic metabolic pathways in bacteria. One of the first examples was demonstrated in the algal polysaccharide-utilizing aerobic planctomycetes producing toxic aldehydes and alcohols from fucose or rhamnose (Erbilgin et al., 2014). Another toxic pathway evolved in the BMC formation is ethanolamine degradation in enteric bacteria and propandiol degradation in anaerobes (Kerfeld et al., 2018; Kennedy et al., 2021). The same locus is also present in the genomes of *Poriferisphaera* and *Mucisphaera*, but not in the other genera of *Phycisphaeraceae*. The physiological significance of this genomic potential for these bacteria as yet not clear as none of them utilize abovementioned substrates inducing formation of the BMC.

Conclusion

Overall, strain AB-hyl4 represents the first example of a natronophilic *Planctomycetota* isolated from a soda lake habitat. Furthermore, to our knowledge, the potential to utilize Hyl as a sole carbon and energy source for growth has never been reported in the characterized members of *Planctomycetota*. Also important to stress that genomic analysis do not support early conclusions on the absence of peptidoglycan in genera belonging to the family *Phycisphaeraceae*, while also showing that at least two out of its four already described genera might be able to form microcompartments (encapsulins) to segregate toxic metabolites from aerobic sugar metabolism.

On the basis of distant phylogenomic and unique phenotypic properties, the soda lake planctomycetes strain AB-hyl4 is proposed to form a new genus and species *Natronomicrosphaera hydrolytica* gen, nov., sp. nov., within the family *Phycisphaeraceae*. The new genus and species protologues are presented in Table 5.

CRediT authorship contribution statement

Dimitry Y. Sorokin: Writing – original draft, Methodology, Investigation, Funding acquisition, Conceptualization. **Alexander Y. Merkel:** Writing – original draft, Methodology, Investigation. **Nicole J. Bale:** Writing – original draft, Investigation. **Michel Koenen:** Investigation. **Jaap S. Sinninghe Damsté:** Writing – review & editing. **Laura Marturano:** Investigation. **Enzo Messina:** Investigation. **Violetta La Cono:** Investigation. **Michail M. Yakimov:** Writing – review & editing, Writing – original draft, Supervision, Investigation, Conceptualization.

Funding information

DYS and AYM were supported by the Russian Ministry of Higher Education and Science. DYS also received support from the Russian Science Foundation (grant 25–14-00272). The work of LM, MMY and VLC were funded by the National Council of Research (CNR) and the Vietnamese Academy of Science and Technology (VAST) in the framework of two bilaterally collaborative projects, EXPLO-Halo and HaloPharm, under grant numbers QTIT01.01/20–21 and QTIT01.01/23–24, respectively.

Declaration of competing interest

The authors declare that they have no known competing financial interests or personal relationships that could have appeared to influence the work reported in this paper.

Acknowledgments

Denise Dorhout and Monique Verweij are acknowledged for their technical support with analysis of intact polar lipids.

Appendix A. Supplementary data

Supplementary data to this article can be found online at https://doi.org/10.1016/j.syapm.2025.126608.

Data availability

Data will be made available on request.

References

Altschul, S.F., Madden, T.L., Schäffer, A.A., Zhang, J., Zhang, Z., Miller, W., et al., 1997. Gapped BLAST and PSI-BLAST: a new generation of protein database search programs. Nucleic Acids Res. 25, 3389–3402.
Anisimova, M., Gascuel, O., 2006. Approximate likelihood-ratio test for branches: a fast, accurate, and powerful alternative. Syst. Biol. 55, 539–552.
Armstrong, Z., Rahfeld, P., Withers, S.G., 2017. Discovery of new glycosidases from metagenomic libraries. Methods Enzymol. 597, 3–23.
Bains, R.K., Nasseri, S.A., Liu, F., Wardman, J.F., Rahfeld, P., Withers, S.G., 2023. Characterization of a new family of 6-sulfo-N-acetylglucosaminidases. J. Biol. Chem. 299, 105214.
Bale, N.J., Rijpstra, W.I.C., Oshkin, I.Y., Belova, S.E., Dedysh, S.N., Sinninghe Damsté, J. S., 2019. Fatty acid and hopanoid adaption to cold in the methanotroph *Methylovulum psychrotolerans*. Front. Microbiol. 10, 589.
Bale, N.J., Ding, S., Hopmans, E.C., Villanueva, L., Boschman, R.C., 2021. Lipidomics of environmental microbial communities. I: visualization of specific niches using untargeted analysis of high-resolution mass spectrometry data. Front. Microbiol. 12, 659302.
Barabote, R.D., Saier, M.H., 2005. Comparative genomic analyses of the bacterial phosphotransferase system. Microbiol. Mol. Biol. Rev. 69, 608–634.
Benito-Arenas, R., Zárate, S.G., Revuelta, J., Bastida, A., 2019. Chondroitin sulfate-degrading enzymes as tools for the development of new pharmaceuticals. Catalysts 9, 322.
Blanvillain, S., Meyer, D., Boulanger, A., Lautier, M., Guynet, C., Denancé, N., et al., 2007. Plant carbohydrate scavenging through tonB-dependent receptors: a feature shared by phytopathogenic and aquatic bacteria. PLoS One 2, e224.
Buckel, W., 2001. Sodium ion-translocating decarboxylases. Biochim. Biophys. Acta 1505, 15–27.
Capella-Gutiérrez, S., Silla-Martínez, J.M., Gabaldón, T., 2009. trimAl: a tool for automated alignment trimming in large-scale phylogenetic analyses. Bioinformatics (Oxford, England) 25, 1972–1973.
Chaumeil, P.A., Mussig, A.J., Hugenholtz, P., Parks, D.H., 2022. GTDB-Tk v2: memory friendly classification with the genome taxonomy database. Bioinformatics (Oxford, England) 38, 5315–5316.
Chen, Y.H., Cheng, W.H., 2024. Hexosamine biosynthesis and related pathways, protein N-glycosylation and O-GlcNAcylation: their interconnection and role in plants. Front. Plant Sci. 15, 1349064.
Dong, J., Cui, Y., Qu, X., 2024. Metabolism mechanism of glycosaminoglycans by the gut microbiota: Bacteroides and lactic acid bacteria: a review. Carbohydr. Polym. 332, 121905.
Drula, E., Garron, M.L., Dogan, S., Lombard, V., Henrissat, B., Terrapon, N., 2022. The carbohydrate-active enzyme database: functions and literature. Nucleic Acids Res. 50, D571–D577.
Elcheninov, A.G., Ugolkov, Y.A., Elizarov, I.M., Klyukina, A.A., Kublanov, I.V., Sorokin, D.Y., 2023. Cellulose metabolism in halo(natrono)archaea: a comparative genomics study. Front. Microbiol. 14, 1112247.
Erbilgin, O., McDonald, K.L., Kerfeld, C.A., 2014. Characterization of a planctomycetal organelle: a novel bacterial microcompartment for the aerobic degradation of plant saccharides. Appl. Environ. Microbiol. 80, 2193–2205.
Fukunaga, Y., Kurahashi, M., Sakiyama, Y., Ohuchi, M., Yokota, A., Harayama, S., 2009. *Phycisphaera mikurensis* gen. Nov., sp. nov., isolated from a marine alga, and proposal of *Phycisphaeraceae* fam. Nov., *Phycisphaerales* Ord. Nov. and *Phycisphaerae* classis nov. in the phylum *Planctomycetes*. J. Gen. Appl. Microbiol. 55, 267–275.
Grant, B.D., Jones, B.E., 2016. Bacteria, archaea and viruses of soda lakes. In: soda lakes of East Africa, M. Schagerl (ed); springer international publishing, Switzerland, pp. 97-147.
Haines, T.H., 2001. Do sterols reduce proton and sodium leaks through lipid bilayers? Prog. Lipid Res. 40, 299–324.
Haines, M., Khot, V., Strous, M., 2023. The vigor, futility and application of microbial element cycling in alkaline soda lakes. Elements 19, 30–36.
Hameleers, L., Pijning, T., Gray, B.B., Fauré, R., Jurak, E., 2024. Novel β-galactosidase activity and first crystal structure of glycoside hydrolase family 154. New Biotechnol. 80, 1–11.

Hashimoto, W., Kobayashi, E., Nankai, H., Sato, N., Miya, T., Kawai, S., Murata, K., 1999. Unsaturated glucuronyl hydrolase of Bacillus sp. GL1: novel enzyme prerequisite for metabolism of unsaturated oligosaccharides produced by polysaccharide lyases. Arch. Biochem. Biophys. 368, 367–374.
Higgins, M.A., Tegl, G., Macdonald, S.S., Arnal, G., Brumer, H., Withers, S.G., et al., 2021. *N*-glycan degradation pathways in gut- and soil-dwelling *Actinobacteria* share common core genes. ACS Chem. Biol. 16, 701–711.
Hovingh, P., Linker, A., 1999. Hyaluronidase activity in leeches (Hirudinea). Comp. Biochem. Physiol. B Biochem. Mol. Biol. 124, 319–326.
Huang, W., Lunin, V., Li, Y., Suzuki, S., Sugiura, N., Miyazono, H., et al., 2003. Crystal structure of *Proteus vulgaris* chondroitin sulfate ABC lyase I at 1.9 Å resolution. J. Mol. Biol. 328 (3), 623–634.
Itoh, T., Hashimoto, W., Mikami, B., Murata, K., 2006. Crystal structure of unsaturated glucuronyl hydrolase complexed with substrate molecular insights into its catalytic reaction mechanism. J. Biol. Chem. 281, 29807–29816.
Jedrzejas, M.J., 2007. Unveiling molecular mechanisms of bacterial surface proteins: *Streptococcus pneumoniae* as a model organism for structural studies. Cell. Mol. Life Sci. 64, 2799–2822.
Jedrzejas, M.J., Mello, L.V., de Groot, B.L., Li, S., 2002. Mechanism of hyaluronan degradation by *Streptococcus pneumoniae* hyaluronate lyase: structures of complexes with the substrate. J. Biol. Chem. 277, 28287–28297.
Jones, B.F., Eugste, R.H.P., Rettig, S.L., 1977. Hydrochemistry of the Lake Magadi basin. Kenya. Geochim. Cosmochim. Acta 41, 53–72.
Kallscheuer, N., Wiegand, S., Kohn, T., Boedeker, C., Jeske, O., Rast, P., 2020. Cultivation-independent analysis of the bacterial community associated with the calcareous sponge *Clathrina clathrus* and isolation of *Poriferisphaera* Corsica gen. Nov., sp. nov., belonging to the barely studied class *Phycisphaerae* in the phylum *Planctomycetes*. Front. Microbiol. 11, 602250.
Kalyaanamoorthy, S., Minh, B.Q., Wong, T., von Haeseler, A., Jermiin, L.S., 2017. ModelFinder: fast model selection for accurate phylogenetic estimates. Nat. Methods 14, 587–589.
Kennedy, N.W., Mills, C.E., Nichols, T.M., Abrahamson, C.H., Tullman-Ercek, D., 2021. Bacterial microcompartments: tiny organelles with big potential. Curr. Opin. Microbiol. 63, 36–42.
Kerfeld, C.A., Aussignargues, C., Zarzycki, J., Cai, F., Sutter, M., 2018. Bacterial microcompartments. Nat. Rev. Microbiol. 16, 277–290.
Kim, D., Park, S., Chun, J., 2021. Introducing EzAAI: a pipeline for high throughput calculations of prokaryotic average amino acid identity. J. Microbiol. (Seoul, Korea) 59, 476–480.
Kulichevskaya, I.S., Ivanova, A.A., Baulina, O.I., Rijpstra, W.I.C., Sinninghe Damsté, J.S., Dedysh, S.N., 2017. *Fimbriiglobus ruber* gen. Nov., sp. nov., a *Gemmata*-like planctomycete from *Sphagnum* peat bog and the proposal of Gemmataceae fam. Nov. Int. J. Syst. Evol. Microbiol. 67, 218–224.
Kumar, S., Stecher, G., Li, M., Knyaz, C., Tamura, K., 2018. MEGA X: molecular evolutionary genetics analysis across computing platforms. Mol. Biol. Evol. 35, 1547–1549.
Lagkouvardos, I., Joseph, D., Kapfhammer, M., Giritli, S., Horn, M., Haller, D., et al., 2016. IMNGS: a comprehensive open resource of processed 16S rRNA microbial profiles for ecology and diversity studies. Sci. Rep. 6, 33721.
Li, S., Jedrzejas, M.J., 2001. Hyaluronan binding and degradation by *Streptococcus agalactiae* hyaluronate lyase. J. Biol. Chem. 276, 41407–41416.
Lombard, V., Ramulu, H.G., Drula, E., Coutinho, P.M., Henrissat, B., 2014. The carbohydrate-active enzymes database (CAZy) in 2013. Nucleic Acids Res. 42, D490–D495.
Lowry, O.H., Rosebrough, N.J., Farr, A.L., Randall, R.J., 1951. Protein measurement with Folin phenol reagent. J. Biol. Chem. 193, 265–275.
Marchler-Bauer, A., Bo, Y., Han, L., He, J., Lanczycki, C.J., Lu, S., et al., 2017. CDD/SPARCLE: functional classification of proteins via subfamily domain architectures. Nucleic Acids Res. 45, D200–D203.
Minh, B.Q., Nguyen, M.A., von Haeseler, A., 2013. Ultrafast approximation for phylogenetic bootstrap. Mol. Biol. Evol. 30, 1188–1195.
Minh, B.Q., Schmidt, H.A., Chernomor, O., Schrempf, D., Woodhams, M.D., von Haeseler, A., Lanfear, R., 2020. IQ-TREE 2: new models and efficient methods for phylogenetic inference in the genomic era. Mol. Biol. Evol. 37, 1530–1534.
Mitchell, A.L., Attwood, T.K., Babbitt, P.C., Blum, M., Bork, P., Bridge, A., et al., 2019. InterPro in 2019: improving coverage, classification and access to protein sequence annotations. Nucleic Acids Res. 47, D351–D360.
Oiki, S., Mikami, B., Maruyama, Y., Murata, K., Hashimoto, W., 2017. A bacterial ABC transporter enables import of mammalian host glycosaminoglycans. Sci. Rep. 7, 1069.
Parks, D.H., Chuvochina, M., Waite, D.W., Rinke, C., Skarshewski, A., Chaumeil, P.A., Hugenholtz, P., 2018. A standardized bacterial taxonomy based on genome phylogeny substantially revises the tree of life. Nat. Biotechnol. 36, 996–1004.
Pfennig, N., Lippert, K.D., 1966. Über das Vitamin B12-Bedürfnis phototropher Schwefelbakterien. Arch. Mikrobiol. 55, 245–256.
Pradel, N., Fardeau, M.-L., Tindall, B.J., Spring, S., 2020. *Anaerohalosphaera lusitana* gen. Nov., sp. nov., and *Limihaloglobus sulfuriphilus* gen. Nov., sp. nov., isolated from solar saltern sediments, and proposal of *Anaerohalosphaeraceae* fam. Nov. within the order *Sedimentisphaerales*. Int. J. Syst. Evol. Microbiol. 70, 1321–1330.
Pritchard, L., Glover, R.H., Humphris, S., Elphinstone, J.G., Toth, I.K., 2016. Genomics and taxonomy in diagnostics for food security: soft-rotting enterobacterial plant pathogens. Anal. Methods 8, 12–24.
Quast, C., Pruesse, E., Yilmaz, P., Gerken, J., Schweer, T., Yarza, P., Peplies, J., Glöckner, F.O., 2013. The SILVA ribosomal RNA gene database project: improved data processing and web-based tools. Nucleic Acids Res. 41, D590–D596.
Reynolds, E.S., 1963. The use of lead citrate at high pH as an electron-opaque stain in electron microscopy. J. Cell Biol. 17, 208–213.
Rinke, C., Chuvochina, M., Mussig, A.J., Chaumeil, P.-A., Davín, A.A., Waite, D.W., Whitman, W.B., Parks, D.H., Hugenholtz, P., 2021. A standardized archaeal taxonomy for the genome taxonomy database. Nat. Microbiol. 6, 946–959.
Sagota, B., Gaysinski, M., Mehiric, M., Guigonis, J.-M., Le Ruduliera, D., Alloinga, G., 2010. Osmotically induced synthesis of the dipeptide *N*-acetylglutaminylglutamine amide is mediated by a new pathway conserved among bacteria. PNAS 107, 12652–12657.
Schagerl, M. (Ed.), 2016. Soda Lakes of East Africa. Springer International Publishing, Switzerland, p. 407.
Senni, K., Pereira, J., Gueniche, F., Delbarre-Ladrat, C., Sinquin, C., Ratiskol, J., et al., 2011. Marine polysaccharides: a source of bioactive molecules for cell therapy and tissue engineering. Mar. Drugs 9, 1664–1681.
Sinninghe Damsté, J.S., Rijpstra, W.I.C., Schouten, S., Fuerst, J.A., Jetten, M.S.M., Strous, M., 2004. The occurrence of hopanoids in planctomycetes: implications for the sedimentary biomarker record. Org. Geochem. 35, 561–566.
Sorokin, D.Y., 2017. Anaerobic haloalkaliphiles. In: Encyclopedia Life Science. John Wiley&Sons, Ltd:Chichester. https://doi.org/10.1002/9780470015902.a0027654.
Sorokin, D.Y., Berben, T., Melton, E.D., Overmars, L., Vavourakis, C., Muyzer, G., 2014. Microbial diversity and biogeochemical cycling in soda lakes. Extremophiles 18, 791–809.
Sorokin, D.Y., Banciu, H.A., Muyzer, G., 2015a. Functional microbiology of soda lakes. Curr. Opin. Microbiol. 25, 88–96.
Sorokin, D.Y., Toshchakov, S.V., Kolganova, T.V., Kublanov, I.V., 2015b. Halo(natrono) archaea isolated from hypersaline lakes utilize cellulose and chitin as growth substrates. Front. Microbiol. 6, 942.
Sorokin, D.Y., Khijniak, T.V., Kostrikina, N.A., Elcheninov, A.G., Toshchakov, S.V., Bale, N.J., et al., 2018. *Natronobiforma cellulositropha* gen. Nov., sp. nov., a novel haloalkaliphilic member of the family *Natrialbaceae* (class *Halobacteria*) from hypersaline alkaline lakes. Syst. Appl. Microbiol. 41, 355–362.
Sorokin, D.Y., Elcheninov, A.G., Toshchakov, S.V., Bale, N.J., Sinninghe Damsté, J.S., Khijniak, T.V., et al., 2019. *Natrarchaeobius chitinivorans* gen. Nov., sp. nov., and *Natrarchaeobius halalkaliphilus* sp. nov., alkaliphilic, chitin-utilizing haloarchaea from hypersaline alkaline lakes. Syst. Appl. Microbiol. 42, 309–318.
Stern, R., Jedrzejas, M.J., 2006. Hyaluronidases: their genomics, structures, and mechanisms of action. Chem. Rev. 106, 818–839.
Tatusova, T., DiCuccio, M., Badretdin, A., Chetvernin, V., Nawrocki, E.P., Zaslavsky, L., Lomsadze, A., Pruitt, K.D., Borodovsky, M., Ostell, J., 2016. NCBI prokaryotic genome annotation pipeline. Nucleic Acids Res. 44, 6614–6624.
Teufel, F., Almagro Armenteros, J.J., Johansen, A.R., et al., 2022. SignalP 6.0 predicts all five types of signal peptides using protein language models. Nat. Biotechnol. 40, 1023–1025.
Uritskiy, G.V., DiRuggiero, J., Taylor, J., 2018. MetaWRAP - a flexible pipeline for genome-resolved metagenomic data analysis. Microbiome 6, 158.
Vavourakis, C.D., Ghai, R., Rodriguez-Valera, F., Sorokin, D.Y., Tringe, S.G., Hugenholtz, P., et al., 2016. Metagenomic insights into the microbial community structure and function of hypersaline soda lake brines. Front. Microbiol. 7, 211.
Vavourakis, C.D., Andrei, A.S., Mehrshad, M., Ghai, R., Sorokin, D.Y., Muyzer, G., 2018. A metagenomics roadmap to the uncultured genome diversity in hypersaline soda lake sediments. Microbiome 6, 168.
Vavourakis, C.D., Mehrshad, M., Balkema, C., van Hall, R., Andrei, A.Ş., Ghai, R., Sorokin, D.Y., Muyzer, G., 2019. Metagenomes and metatranscriptomes shed new light on the microbial-mediated sulfur cycle in a Siberian soda lake. BMC Biol. 17, 69.
Wang, W., Wang, J., Li, F., 2017. Hyaluronidase and chondroitinase. Adv. Exp. Med. Biol.: Protein Rev. 17, 75–87.
Wang, X., Wei, Z., Wu, H., Li, Y., Han, F., Yu, W., 2021. Characterization of a hyaluronic acid utilization locus and identification of two hyaluronate lyases in a marine bacterium *vibrio alginolyticus* LWW-9. Front. Microbiol. 2021 (12), 69609.
Wang, L., Liu, Q., Gong, X., Jian, W., Cui, Y., Jia, Q., et al., 2022. Cloning and biochemical characterization of a hyaluronate lyase from Bacillus sp. CQMU-D. J. Microbiol. Biotechnol. 33, 235.
Wang, J., Chitsaz, F., Derbyshire, M.K., Gonzales, N.R., Gwadz, M., Lu, S., et al., 2023. The conserved domain database in 2023. Nucleic Acids Res. 51 (D1), D384–D388.
Wick, R.R., Judd, L.M., Gorrie, C.L., Holt, K.E., 2017. Unicycler: resolving bacterial genome assemblies from short and long sequencing reads. PLoS Computational Biol. 13, e1005595.
Yasuda, T., 2011. Hyaluronan inhibits Akt, leading to nuclear factor-κB down-regulation in lipopolysaccharide-stimulated U937 macrophages. J. Pharmacol. Sci. 115, 509–515.
Yoon, J., Jang, J.-H., Kasai, H., 2014. *Algisphaera agarilytica* gen. Nov., sp. nov., a novel representative of the class *Phycisphaerae* within the phylum *Planctomycetes* isolated from a marine alga. Antonie Van Leeuwenhoek 105, 317–324.
Zhang, L., Jiang, J., Liu, W., Wang, L., Yao, Z., Li, H., et al., 2024. Identification and characterization of a highly active hyaluronan lyase from *Enterobacter asburiae*. Mar. Drugs 22, 399.
Zheng, J., Ge, Q., Yan, Y., Zhang, X., Huang, L., Yin, Y., 2023. dbCAN3: automated carbohydrate-active enzyme and substrate annotation. Nucleic Acids Res. 51, W115–W121.
Zorz, J.K., Sharp, C., Kleiner, M., Gordon, P.M.K., Pon, R.T., Dong, X., et al., 2019. A shared core microbiome in soda lakes separated by large distances. Nat. Commun. 10, 4230.

Natronomicrosphaera hydrolytica, gen. nov., **sp. nov.***, a first representative of the phylum Planctomycetota from soda lakes*

Dimitry Y. Sorokin, Alexander Y. Merkel, Nicole J. Bale, Michel Koenen, Jaap S. Sinninghe Damsté, Laura Marturano, Enzo Messina, Violetta La Cono and Michail M. Yakimov

Supplementary data

Table S1. Genome statistics of strain AB-hyl4 and its closest related MAGs from the same habitat (Kulunda Steppe Cock Soda Lake)

Table S2. Carbohydrate-active enzymes found in the strain AB-hyl4 genome with the dbCAN and Signal 6.0 servers.

Table S1

Parameter	**AB-hyl4**	MAG CSSed162cmA_392	MAG CSSed162cmB_538
GenBank assembly	GCA_041821185	GCA_007119405	GCA_007125385
Genome size	4.6 Mbp	3.3 Mb	4.8 Mb
Number of contigs	32	669	762
GC percent	62.5	69	68.5
Contig N50	429.5 kb	5.2 kb	7.3 kb
Genome coverage	1000	13	16
Genes (total)	3931	2964	4279
CDSs (with protein)	3826	2920	4188
RNA genes	53	24	41
rRNAs	1, 1, 1 (5S, 16S, 23S)	1 (16S)	1 (23S)
complete rRNAs	1, 1, 1 (5S, 16S, 23S)	-	-
tRNAs	47	21	37
Pseudo Genes (total)	52	20	50
Completeness (checkm2), %	96.99	56.53	72.45
Contamination (checkm2), %	1,1	1.6	2.32
Completeness (checkm), %	95.45	63.95	70.36
Contamination (checkm), %	1,14	0.00	1.70

Table S2.

Protein_id	CAZy family	% ident	length	protein	Signal Peptide	Closest hit
MFA9476674	GH78	41	765	alpha-L-rhamnosidase	No	ACZ43235
MFA9476682	GH106	42	1048	glycosyl hydrolase	No	WYJ07678
MFA9476688	GH130_7	66	343	glycosyl hydrolase	No	WDM29354
MFA9476694	GH4	70	498	alpha-glucosidase/alpha-galactosidase	No	QQE11541
MFA9476741	GH0	59	749	DUF4965 domain	No	QQE13087
MFA9476800	GH57	65	391	polysaccharide deacetylase	No	QOV88508
MFA9476841	GH9	41	621	DUF255 domain	No	ULQ52457
MFA9477378	GH130_2	70	314	glycosyl hydrolase	No	QUI23662
MFA9477592	GH15	66	731	glycosyl hydrolase	No	QDU71278
MFA9477724	GH130_8	63	504	glycosyl hydrolase	No	QDU34727
MFA9477817	GH89	39	698	alpha-N-acetylglucosaminidase	No	QJD79315
MFA9477843	GH88	70	441	glycosyl hydrolase	No	AMP57235
MFA9477920	GH0	44	482	trehalase family glycosidase	No	AJY75338
MFA9477926	GH116	57	820	glycosyl hydrolase	No	WCJ58802
MFA9477928	GH2	33	796	glycosyl hydrolase	No	WLT30908
MFA9477931	GH172	68	372	glycosyl hydrolase	No	AUS95664
MFA9477949	GH140	54	442	glycosyl hydrolase	No	QOY88013
MFA9478056	GH0	40	665	DUF4838 domain	No	UCI13013
MFA9478067	GH123	30	815	glycosyl hydrolase	Sec/SPI	AVM44861
MFA9478084	GH78	44	922	glycosyl hydrolase	No	QIN81509
MFA9478089	GH78	47	543	alpha-L-rhamnosidase	No	ARN57683
MFA9478098	GH151	54	659	alpha-amylase	No	QYY36370
MFA9478115	GH38	41	1087	alpha-mannosidase	No	CCW34438
MFA9478116	GH2	48	393	GH71/99-like	Tat/SPI	ANU64886.2
MFA9478215	GH130_4	56	355	glycosyl hydrolase	No	QQE12332
MFA9478480	CBM67, GH78	40	727	alpha-L-rhamnosidase	No	WPJ96098
MFA9478583	GH38	37	939	glycosyl hydrolase	No	UVI33384
MFA9478585	GH172	71	375	glycosyl hydrolase	No	BCM94094
MFA9478588	GH106	40	1041	glycosyl hydrolase	No	WYJ07678
MFA9478724	GH4	56	461	glycosyl hydrolase	No	WDH96367
MFA9478739	GH0	62	513	GH35, endo-1,4-beta-xylanase	No	QDU33627

MFA9478761	GH89	47	745	alpha-N-acetylglucosaminidase	No	BBL05600
MFA9478814	GH2	43	948	glycosyl hydrolase	No	ASA21598
MFA9478847	GH0	42	638	DUF4838 domain	Sec/SPI	UCI13013
MFA9478866	GH38	30	1004	glycosyl hydrolase	No	XBV87194
MFA9479081	GH151	40	653	glycosyl hydrolase	No	QEH34392
MFA9479185	GH0	63	904	glucosidase	No	CUQ65639
MFA9479236	GH151	55	665	beta-galactosidase	No	AEE97446
MFA9479308	PL8_2	31	927	chondroitinase family	Sec/SPI	UQZ84194
MFA9479315	GH130_7	60	338	glycosyl hydrolase	No	WNR45545
MFA9479336	GH0	37	661	DUF4838 domain	Sec/SPI	QYM78553
MFA9479648	GH133	47	750	amylo-alpha-1,6-glucosidase	No	QQE13629
MFA9479697	CBM48, GH13_8	68	669	alpha-amylase family	No	QOV88287
MFA9479771	GH2	55	682	beta-galactosidase	No	BDG36489
MFA9479976	GH2	61	789	beta-galactosidase	No	UQZ85313
MFA9479979	GH0	37	655	DUF4838 domain	No	QOV87612
MFA9479984	GH78	41	806	alpha-L-rhamnosidase	No	QYM79363
MFA9480030	GH0	36	645	DUF4838 domain	No	UCI13013
MFA9480048	GH0	37	649	DUF4838 domain	Sec/SPII	UCI13013
MFA9480067	GH78	56	894	alpha-L-rhamnosidase	No	ABQ91107
MFA9480320	GH105	54	362	unsaturated glucuronate hydrolase	No	UFU07376
MFA9480364	GH78	44	589	alpha-L-rhamnosidase	No	ACZ43235
MFA9480427	GH20	43	508	beta-N-acetylhexosaminidase	No	QDU70463
MFA9480464	GH35	47	944	beta-galactosidase	No	XAM00319